

1 **Strong changes in englacial temperatures despite insignificant changes in ice thickness**  
2 **at Dôme du Goûter glacier (Mont-Blanc area)**

3  
4 *Christian Vincent<sup>1</sup>, Adrien Gilbert<sup>1</sup>, Bruno Jourdain<sup>1</sup>, Luc Piard<sup>1</sup>, Patrick Ginot<sup>1</sup>, Vladimir*  
5 *Mikhalenko<sup>2</sup>, Philippe Possenti<sup>1</sup>, Emmanuel Le Meur<sup>1</sup>, Olivier Laarman<sup>1</sup> and Delphine Six<sup>1</sup>*

6  
7 *(1) Univ. Grenoble Alpes, CNRS, IRD, Grenoble INP, IGE, 38000 Grenoble, France.*

8 *(2) Institute of Geography, Russian Academy of Sciences*

9  
10 **Abstract**

11  
12 The response of very high elevation glaciated areas on Mont Blanc to climate change has been  
13 analyzed using observations and numerical modeling over the last two decades. Unlike the changes at  
14 low elevations, we observe very low glacier thickness changes, of about -2.6 m on the average since  
15 1993. The slight changes in horizontal ice flow velocities and submergence velocities suggest a  
16 decrease of about 10 % in ice flux and surface mass balance. This is due to less snow accumulation  
17 and is consistent with the precipitation decrease observed in meteorological data. Conversely,  
18 measurements performed in deep boreholes since 1994 reveal strong changes in englacial temperature  
19 reaching 1.5 °C increase at a depth of 50 m. We conclude that at such very high elevations, current  
20 changes in climate do not lead to visible changes in glacier thickness but cause invisible changes  
21 within the glacier in terms of englacial temperatures. Our analysis from numerical modeling shows  
22 that glacier near-surface temperature warming is enhanced by increasing melt-frequency at high  
23 elevations although the impact on surface mass balance is low. This results in a non-linear response of  
24 englacial temperature to currently rising air temperatures. In addition, borehole temperature inversion  
25 including a new dataset confirms previous findings of similar air temperature changes at high and low  
26 elevations in the Alps.

27  
28 **1. Introduction**

29  
30 Glaciers are very sensitive to climate change, as shown by numerous studies (e.g. Oerlemans, 2001;  
31 Huss, 2012; Thibert et al., 2018). Over recent decades, they have become one of the most emblematic  
32 indicators of climate change for the general public. Many glaciers in the world have strongly receded  
33 over recent decades (Zemp et al., 2019; Gardner et al., 2013). However, the sensitivity of mass balance  
34 to climate can be very different depending on the climatic region and meteorological conditions  
35 (Oerlemans, 2001). In addition, the influence of climate change on the surface mass balance depends  
36 strongly on elevation (Vincent et al., 2007a). Due to the difficulty of access, very few measurements

37 have been carried out on glaciers at very high elevations (WGMS, 2015) even though englacial  
38 temperatures and surface mass balance are amongst the few indicators of climate change at such very  
39 high elevations. Englacial temperatures in these cold areas are very sensitive to atmospheric change  
40 due the associated increase in surface melting. Gilbert et al. (2014a) showed that the enhanced uptake  
41 of energy at the surface of cold glaciers is triggered by the increasing energy flux from the atmosphere  
42 due to surface energy balance when surface temperatures reach 0°C. Percolation and refreezing  
43 processes efficiently transfer this energy from the surface to underlying layers.  
44 In the Alps, most of the observations of mass balance have been carried out on low-altitude glaciers,  
45 generally below 3600 m above sea level (a.s.l.) (WGMS, 2015). Most of these glaciers are temperate.  
46 Consequently, an increase in surface energy balance leads to an increase in melting. The processes are  
47 different for cold glaciers at very high elevations for which an excess of energy balance at the surface  
48 results mainly in englacial temperature increase (Hutter, 1983; Aschwanden and Blatter, 2009).  
49 Englacial temperature measurements are available for very few cold alpine glaciers at high elevations  
50 (Lüthi and Funk, 2000; Suter, 2002; Hoelzle et al., 2011; Vincent et al., 2007b; Gilbert et al., 2010;  
51 Gilbert and Vincent, 2013). Even fewer measurements are available at these elevations to  
52 simultaneously assess changes in both surface mass balance and englacial temperatures. Our study  
53 aims to jointly assess surface mass balance and englacial temperature changes at very high elevation  
54 over 25 years (1993-2017) from in-situ measurements at Col du Dôme (4250 m), French Alps, to  
55 study the impact of climate change on such high-elevation glaciated areas.

56

## 57 **2. Study site and data**

58

59 The Dôme du Goûter is located in the Mont Blanc area at an elevation of 4300 m a.s.l, 7 km from  
60 Chamonix Mont-Blanc. It is a small ice cap with ice thickness ranging from 45 to 140 m (Vincent et  
61 al., 2007b). Three hundred meters from the summit, there is a saddle with very gentle slopes, named  
62 Col du Dôme (4250 m a.s.l.). On this saddle, four deep boreholes down to about 126 m deep have  
63 been drilled since 1994 at the same location, within a radius of several meters.

64

### 65 **2.1 Englacial temperature measurements**

66

67 Englacial temperatures were measured from surface to bedrock at the same location (red triangle in  
68 Figure 1) using thermistor chains in deep boreholes. Boreholes were drilled electromechanically in  
69 1994, 2004 and 2016. The 2010 borehole was drilled using hot water. Thermistors with 0.05 °C  
70 accuracy were installed in all boreholes after drilling. In 1994, temperatures were measured 3 days  
71 after drilling. In 2004, temperatures were measured 5 days after drilling and again 6 months later. In  
72 2010 and 2016, temperatures were measured several times during 6 and 7 months respectively after  
73 drilling. Except in 1994, measurements were repeated several times in each borehole until a thermal

74 equilibrium ( $\pm 0.05$  °C) was reached. Indeed, repeated measurements after drilling and after several  
75 weeks or months show that the borehole temperatures below 20 m deep are consistent ( $\pm 0.05$  °C). The  
76 accuracy of measurements performed in 1994 is assessed to be better than  $\pm 0.1$  °C. Density profiles  
77 were measured along the ice cores extracted in 1994 and in 2012. Note that the englacial temperatures  
78 have been measured between the surface and 73 m deep only in the borehole of 2012 and are not used  
79 in this study.

80

## 81 **2.2 Ice-flow velocities and geodetic measurements**

82

83 Horizontal velocities have been obtained from the position of the lowest part of accumulation stakes  
84 buried deep in snow, 5 m long and 10 cm in diameter, considering the tilt and orientation of the stakes  
85 (Vincent et al., 2007a). Depending on the accumulation rate, the stakes were buried by snow every 6  
86 months or every year. Twenty stakes were distributed in 1997 in the area shown in Figure 1. These  
87 stakes were replaced only in 1998, 1999, 2002, 2003, 2004, 2008, 2009 and 2016. Consequently, the  
88 series of ice-flow velocities and accumulation measurements are not continuous in time. In addition,  
89 the stake locations were modified over the period 1997-2004 (Vincent et al., 2007a). From 2009 to  
90 2017, a fixed network of 12 stakes was used, with the stakes always at the same locations, however the  
91 measurements were not continuous over this period. The ice-flow velocities have been calculated and  
92 averaged over 3 time periods (1997-2004, 2009-2011, 2016-2017). The theodolite-based field methods  
93 used to obtain surface velocity and surface topography data before 2000 have been fully described by  
94 Vincent et al. (1997). After 2000, geodetic measurements were performed with a Leica 1200  
95 Differential GPS (DGPS) unit running with dual frequencies. Occupation times were typically 1 min  
96 with 1-s sampling and the number of visible satellites (NAVSTAR and GLONASS) was greater than  
97 seven. The distance between the fixed receiver and the mobile receiver was less than 500 m. The  
98 DGPS positions have an intrinsic accuracy of  $\pm 0.01$  m. However, because of the slope and creep of  
99 snow, some stakes tilt with time and, depending on the tilt of the stakes (generally less than  $10^\circ$ ), the  
100 stake horizontal and vertical positions have a maximum uncertainty of  $\pm 0.88$  m and  $\pm 0.09$  m  
101 respectively. Provided that the initial position of the stake is almost vertical ( $\pm 3^\circ$ ), the uncertainty on  
102 horizontal and vertical displacement is assumed to be less than 1 m and 0.1 m respectively. Another  
103 uncertainty could come from a “false” vertical motion due to the warming of the stake from solar  
104 radiation. Given that the stakes are wooden stakes 5 m long and 10 cm in diameter with a low thermal  
105 conductivity and that the temperature of the firn ranges between  $-5$  and  $-15^\circ\text{C}$ , we assume this effect is  
106 negligible. The uncertainties of classical topographic measurements before 1995 are similar to those of  
107 DGPS measurements. The Digital Elevation Models (DEM) were obtained in 1993 and 2017 using the  
108 same in-situ geodetic methods with a grid size of 30 m. The uncertainty obtained for each measured  
109 point of the DEM is  $\pm 0.10$  m and depends mainly on the roughness of the surface. In addition, glacier  
110 thickness changes were measured along a longitudinal cross section over a distance of about 600 m in

111 June 1993, May 1998, October 2003, September 2009, March 2012 and August 2016 in order to  
112 estimate thickness changes over this profile (red line in Figure 1).

113

### 114 **2.3 Ground Penetrating Radar (GPR) measurements**

115

116 Radio echo soundings were made in June 1993 and completed in 1999 on the Dôme du Goûter ice cap  
117 along 12 profiles in order to determine the bedrock topography (Vincent et al., 1997; S. Suter,  
118 unpublished data, 1999). The measurements were performed using a pulse radar transmitter (Icefield  
119 Instruments, Canada) based on the Narod transmitter (Narod and Clarke, 1994) with a frequency of 5  
120 MHz. The speed of electromagnetic wave propagation in the ice was assumed to be identical to the  
121 value of  $175 \mu\text{s}^{-1}$  found at Colle Gnifetti (Wagner, 1994). The field measurements were performed in  
122 such a way as to obtain reflections from the glacier bed located in a vertical plane with the  
123 measurement points at the glacier surface. This makes it possible to locate the glacier bed in 2  
124 dimensions. The bedrock topography was obtained from envelopes of all ellipse functions giving all  
125 the possible reflection positions. The ice thickness in this area ranges from 45 m (Dôme du Goûter) to  
126 140 m (Fig.1).

127

### 128 **2.4 Mass balance and meteorological data**

129

130 In addition to the observations performed at Col du Dome, glaciological and meteorological  
131 observations carried out in the Mont Blanc area have been used in this study. As part of the  
132 GLACIOCLIM observation facility (<https://glacioclim.osug.fr/>), winter and summer surface mass  
133 balances are measured each year on two glaciers in the vicinity of Col du Dome since 1995  
134 (Argentière and Mer de Glace), using the glaciological method (Cuffey and Patterson, 2010). Winter  
135 surface mass balances used in this study are located in the accumulation zone of the glaciers (>3000m)  
136 and are measured at the end of April using snow cores and density measurements. We also used  
137 annual and winter precipitation data from the SAFRAN reanalysis (Système d'Analyse Fournissant  
138 des Renseignements Adaptés à la Nivologie, System of analysis for the provision of information for  
139 the science of snow). This data set is available back to 1958 (Durand and others, 2009). SAFRAN  
140 disaggregates large-scale meteorological analyses and observations in the French Alps. The analyses  
141 provide hourly meteorological data for the Mont-Blanc range, as a function of slope exposures and  
142 altitude (at 300 m intervals). In this study, we used SAFRAN precipitation determined at 4300 m a.s.l.

143

## 144 **3. Results**

145

### 146 **3.1 Surface elevation changes**

147

148 Glacier surface elevation changes were obtained between 1993 and 2017 from DEM comparisons over  
149 a surface area of 0.12 km<sup>2</sup>. As can be seen in Figure 2, the thickness changes are not uniform, showing  
150 both positive and negative values depending on the location on the glacier. In any case, the changes  
151 are small everywhere and do not exceed 7 m between 1993 and 2017. Maximum thinning is located  
152 between the summit of Dôme du Goûter and the pass (Col du Dôme). Conversely, the thickness  
153 change is slightly positive in south-east of this region. Note that the 1 m increase over 24 years found  
154 in this region is small in comparison to annual accumulation which can reach 8 m of snow per year at  
155 some sites and in comparison to interannual accumulation variability which can reach more than 2 m  
156 of snow per year. The average 1993-2017 thickness change obtained over the entire surface area is -  
157 2.65 m.

158 In addition, geodetic measurements were carried out along a longitudinal cross section for different  
159 years (Fig. 3). The measurements were not performed during the same season each year but this is not  
160 crucial given that melting is close to zero at this altitude (Gilbert et al., 2014a) and snow accumulation  
161 occurs throughout the year (Vincent et al., 2007a). Although the measurements were performed on one  
162 longitudinal cross section only, it seems that thickness changes over each period of 5 years are as large  
163 as changes over the whole period of 24 years. From these data, we can conclude that the thickness  
164 changes observed at this altitude over 24 years are very small.

165

### 166 **3.2 Ice flow velocity changes**

167

168 Ice flow velocities were measured at numerous locations before 2009 but not always at the same  
169 locations (Fig. 4). Conversely, after 2009, the number of stakes was reduced but the stakes were  
170 always set up at the same locations. Thanks to the numerous measurements performed between 1997  
171 and 2004, the ice flow velocities have been interpolated over the whole colored area shown in Figure  
172 4. By comparing the velocities measured at similar location during this period, we conclude that the  
173 ice flow velocities did not change significantly between 1997 and 2004.

174 In this way, we can accurately compare the ice flow velocities over three periods, 1997-2004, 2009-  
175 2011 and 2016-2017 at the same locations, i.e. the locations of stakes set up in 2009 and 2016. No  
176 significant change in horizontal ice flow velocities can be detected between the 1997-2004 and 2009-  
177 2011 periods given that the differences are within the uncertainty of measurements (Fig. 5). Between  
178 the 1997-2004 and 2009-2011 periods, the differences are less than 0.86 m a<sup>-1</sup> except for one point  
179 (1.00 m a<sup>-1</sup>). The average of the differences is 0.05 m a<sup>-1</sup> and the standard deviation is 0.52 m a<sup>-1</sup>.  
180 Between the 2009-2011 and 2016-2017 periods, the differences are less than 1 m a<sup>-1</sup> except for 4  
181 points (1.1 and 1.09 m a<sup>-1</sup>). The average of the differences is -0.56 m a<sup>-1</sup> and the standard deviation is  
182 0.43 m a<sup>-1</sup>. Although these differences barely exceed the measurement uncertainty, they are  
183 systematic. Note also that each value results from 3 to 5 topographic surveys, except for the 2016-  
184 2017 period. Therefore, these differences observed between the 2009-2011 and 2016-2017 periods

185 could indicate a deceleration over the last decade. The slope of the regression line between ice-flow  
186 velocities of the 2009-2011 and 2016-2017 periods is 0.92, which means that the ice flow velocity  
187 decreased by 8 %. Over the whole period, using the same method, the ice flow velocity decreased by  
188 11 %. One can conclude that the ice flow velocity changes indicate a change in ice flux very likely  
189 related to surface mass balance changes. Unfortunately, the surface mass balance measurements are  
190 discontinuous. They do not make it possible to detect any temporal change. However, the  
191 submergence velocities can help us to analyze the surface mass balance changes as shown in the next  
192 section.

193

### 194 **3.3 Submergence velocity changes**

195

196 The mean surface mass balance can be analyzed indirectly from the submergence velocities. Previous  
197 studies (Vincent et al., 2007a), have shown that the submergence velocities appear to offer a good way  
198 of assessing the long-term average surface mass balance. Submergence velocities  $w_s$  were calculated  
199 from:

$$200 \quad w_s = w - u \tan \alpha \quad (1)$$

201

202 where  $u$  and  $w$  are the measured horizontal and vertical components of the surface velocity obtained  
203 from stake measurements and  $\tan \alpha$  is the surface slope (Hooke, 2005; Cuffey and Paterson, 2010). The  
204 submergence velocities are expressed in meter water equivalent per year (m w.e.  $a^{-1}$ ) calculated using  
205 the density of the firm which is about  $450 \text{ kg m}^{-3}$  (see Supplementary Material). Assuming an  
206 uncertainty of  $\pm 0.05$  for the relative density and  $\pm 0.1 \text{ m}$  for the vertical velocity component, the  
207 uncertainty should not exceed  $0.4 \text{ m w.e. } a^{-1}$ .

208 As in the analysis of the horizontal ice flow velocities, the submergence velocities of the 1997-2004  
209 period have been interpolated over the whole colored area shown in Figure 6. The submergence  
210 velocities can vary from 0.3 to 3.3 m w.e.  $a^{-1}$  depending on the location. This pattern is highly  
211 correlated with the accumulation pattern as shown by Vincent et al. (2007a). The submergence  
212 velocities have been compared over the three periods 1997-2004, 2009-2011 and 2016-2017 (Fig. 7).  
213 The comparison reveals a decrease of the submergence velocities after 2004. Based on the slope of the  
214 regression lines, the submergence velocities decreased by 8 % between the 1997-2004 and 2009-2011  
215 periods and by 10 % between the 2009-2011 and 2016-2017 periods. Between the 2009-2011 and  
216 2016-2017 periods, the average of the differences is  $-0.14 \text{ m w.e. } a^{-1}$  and the standard deviation is  $0.33$   
217  $\text{m w.e. } a^{-1}$ . Over the whole period (1997-2004 / 2016-2017), the average of the differences is  $-0.41$   
218  $\text{m w.e. } a^{-1}$  and the standard deviation is  $0.21 \text{ m w.e. } a^{-1}$ . Although the average difference is close to the  
219 uncertainty, the differences are systematic. According to the slope of the regression line, the  
220 submergence velocities decreased by 21 % over the whole period. Although the uncertainty is high,  
221 these results indicate a decrease of surface mass balances over the whole period. This explains the

222 decrease in ice flow velocities and ice flux. These relative changes in ice flow velocities, ice flux and  
223 surface mass balances are thoroughly discussed in section 4.

224

### 225 **3.4 Englacial temperature changes**

226

227 Englacial temperature were measured down to the bedrock at 126 m deep at the same location between  
228 1994 and 2017 during four drilling campaigns (Fig. 8). Measurements reveal a strong warming of  
229 near-surface temperatures that likely started before 1994 given that the 1994 temperature profile was  
230 already far from steady state conditions (Vincent et al., 2007a). We defined the near-surface  
231 temperature as the 10 m deep averaged temperature. The near-surface firn temperatures depend on  
232 complex mass and energy exchanges at the snow surface but are mainly driven by air temperature and  
233 meltwater refreezing. This near-surface temperature anomaly due to atmospheric warming was  
234 propagated down to the glacier bottom through advective and diffusive processes throughout the  
235 measurement period as shown in Figure 8.

236 Note that between the surface and a depth of 20 m, the englacial temperature is affected by seasonal  
237 fluctuations (Gilbert et al., 2014a). At depths between 50 and 55 m, the englacial temperature changes  
238 are about +1.5 °C over the whole period (Fig. 8). For the deep layers, below 90 m, the englacial  
239 temperature profile does not show any change until after 2005. The warm wave reached the bedrock  
240 between 2005 and 2010. Over the whole period (1994-2017), the temperature change close to the  
241 bedrock (126 m deep) was +0.3 °C, which is larger than the uncertainty of the measurements. Note  
242 that the last temperature profile measured in 2017 revealed a stabilization of the 40 m-depth  
243 temperature compared to the 2005 and 2010 profiles whereas the temperature anomaly continued to  
244 propagate down to the glacier base.

245 From numerical modeling, Gilbert et al. (2014a) showed that near-surface temperature warming can be  
246 explained by increasing surface melting event duration. They successfully modeled the temperature  
247 evolution up to 2010 using Lyon-Bron meteorological daily data (Météo-France station located 200  
248 km west of the glacier) to force their model. The steady state profile was computed from a steady state  
249 surface temperature and is used as the initial profile in 1907 for the model. The steady surface  
250 temperature was tuned to produce the temperature measured in 1994 (Gilbert and Vincent, 2013). In  
251 the present study, we run the same model in order to see if the 40 m-depth temperature stabilization in  
252 2017 can be explained by the temperature change and the ensuing increasing frequency and duration  
253 of melting events. Results show that the englacial temperature change is still successfully modeled  
254 using the same forcing data and parameters (Fig. 8). This means that the 2017 stabilization observed at  
255 a depth of 40 m is a signature of an air temperature warming rate slowdown observed in the Lyon-  
256 Bron climatic data between 1998 and 2015 and well known on a global scale as “the global warming  
257 hiatus” (Meehl et al., 2014). Over the whole temperature profile between 20 and 126 m deep, the  
258 average increase in temperature is 0.93 °C between 1994 and 2017. By integrating the internal energy

259 change ( $\rho C_p \Delta T$ ) over the whole glacier thickness, we estimate that the glacier absorbed  $3.9 \cdot 10^8 \text{ J m}^{-2}$   
260 between the pre-industrial climate (steady state in our simulation) and 2017, where  $\rho$  is the firn density  
261 ( $\text{kg m}^{-3}$ ),  $C_p$  the heat capacity ( $\text{J kg}^{-1} \text{ K}^{-1}$ ) and  $\Delta T$  the measured temperature change (K). This is  
262 equivalent to 1.17 m w.e. of surface melting.

263

### 264 **3.5 Past changes inferred from borehole temperature inversion**

265

266 Although it is not the main objective of our study, we compared climate change at Col du Dôme with  
267 lower elevation observations, in order to update the findings of Gilbert and Vincent (2013) by  
268 including the new temperature profile (measured in 2017) in the inversion procedure. The model is  
269 based on Bayesian inference and is fully described in Gilbert and Vincent (2013). The reconstruction  
270 of the near-surface temperature at the drilling site (Fig. 9a) includes the four temperature profiles  
271 presented here (1994, 2005, 2010 and 2017). It shows a strong and fast change occurring between  
272 1980 and 1998 followed by a stabilization or slight cooling until 2015. Near-surface temperatures are  
273 estimated to be 2.5 degrees warmer than those in the pre-industrial steady state. The atmospheric  
274 temperature reconstruction (Fig. 9b) is based here on the simultaneous inversion of 8 different  
275 temperature profiles: the 4 presented here and 4 others from two different locations (Gilbert and  
276 Vincent, 2013). The englacial temperature measurements sites are shown in Figure 1. Our analysis  
277 confirms that englacial temperature at Col du Dôme showed a break in the warming trend during the  
278 early 2000s, similarly to what was observed at lower elevations in the region and at a global scale.

279

## 280 **4. Discussion**

281

282 The glacier thickness changes observed between 1993 and 2017 are small and non-uniform. Over the  
283 whole area, the average thickness has decreased by 2.65 m which corresponds to a reduction of 2.4%  
284 of the thickness over this drainage basin (i.e. 2.65/111 m). Note that this thickness change is very  
285 small compared to the thickness change of 80 to 100 m observed at low altitudes (about 2000 m a.s.l.)  
286 on glaciers in the Mont-Blanc area over the last two decades (Berthier et al., 2014 ; Vincent et al.,  
287 2014). At the flux gate shown in Figure 1, the thickness has decreased by 2 % (i.e. 2.56/131 m). Over  
288 the same period, the surface horizontal ice flow velocities have decreased by 11 % at this flux gate.  
289 Three dimensional modeling with firn specific rheology performed by Gilbert et al. (2014b) shows  
290 that the mean horizontal velocity is 70% of the surface horizontal velocity. The mean horizontal  
291 velocity of the cross section can therefore be estimated to have decreased by 7.7%. Consequently the  
292 ice flux has decreased by about 9.7 % between 1993 and 2017. An independent estimation shows that  
293 the submergence velocities have decreased by 21 % over the whole drainage basin. These independent  
294 results seem to reveal a slight change in surface mass balance over the whole period. According to the  
295 ice flux calculations, the surface mass balance has decreased by about 10 %. The greater change in ice



296 flow velocity compared to the change in thickness is not surprising. Indeed, the glacier is frozen to its  
297 bed and no sliding occurs. According to Glen's law and the laminar flow assumption (Cuffey and  
298 Paterson, 2010, Equation 8.36, p.310), the depth averaged horizontal ice velocity is proportional to  $\alpha^3$   
299 and  $H^4$  and therefore the ice flux to  $\alpha^3$  and  $H^5$ , where  $\alpha$  is the surface slope and  $H$  is the glacier  
300 thickness. This means that, to a first order approximation, the relative change in ice thickness (in %) is  
301 a power 1/5 of the relative flux change or relative change in SMB (in %) in the absence of large slope  
302 changes. Similarly, the relative change in ice flow velocity is a power 4/5 of the relative change in  
303 surface mass balance. Assuming a change of 10 % in surface mass balance, there should be a change  
304 of 2 % in ice thickness and 8 % in ice flow velocity. These estimations are consistent with our  
305 observations. The ice thickness is therefore not very sensitive to surface mass balance. Conversely, the  
306 ice flow velocity is more sensitive and this explains the larger relative changes in ice flow velocities  
307 we observed compared to the changes in thickness.

308 The change in surface mass balance we hardly detected could be related to a change in precipitation  
309 over the last two decades. Indeed, the surface mass balance at these high elevations is driven by  
310 changes in precipitation (Vincent et al., 2007b). We therefore analyzed atmospheric precipitation data  
311 from the SAFRAN (Système d'Analyse Fournissant des Renseignements Adaptés à la Nivologie,  
312 System of analysis for the provision of information for the science of snow) reanalysis available back  
313 to 1958 (Durand et al., 2009) and snow accumulation at lower altitudes from Argentière and Mer de  
314 Glace glaciers. This analysis reveals that annual precipitation has decreased by about 10 % in the Mont  
315 Blanc area over the last two decades (Fig. 10). The snow accumulation rates observed at Argentière  
316 and Mer de Glace glaciers show similar trends although these accumulation rates are related to the  
317 winter season only.

318 A source of uncertainty in submergence velocities is related to the snow density. Indeed, the  
319 submergence velocity calculations require the snow/firn density values over the depth at which the  
320 stakes have been set up. The snow density was not measured for each campaign. For our calculations,  
321 we assumed that the snow density did not change with time. The long term change of the firn density  
322 was assessed from drilling core measurements from holes drilled in 1994 and 2012 (see  
323 Supplementary Material, Figure S1). From these measurements, it can be seen that the snow density  
324 did not change significantly over the first 30 meters deep. It means that the calculated submergence  
325 velocities are not affected. However, we can detect a mean relative density difference of 0.016  
326 between the surface and 65 m deep (Fig. S1) that correspond to the firn accumulated between 1994  
327 and 2012. The modelled average surface melting shows an increase of 0.02 m w.e. a<sup>-1</sup> between 1994  
328 and 2012 compared to the period 1976-1994. For a net annual accumulation of 2.7 m w.e. a<sup>-1</sup>, it would  
329 correspond to an increase of 0.004 in relative density, which is lower than the observed change not  
330 detectable from density measurements. It is therefore unlikely that an increase in melting is  
331 responsible for the observed slight density increase which instead may be related to reduced snow  
332 accumulation.

333 Over the entire 20<sup>th</sup> century, a previous study (Vincent et al., 2007b) showed that the thickness of  
334 glaciers at these high elevations did not change significantly. It suggested that surface accumulation  
335 rates did not change significantly over the entire 20<sup>th</sup> century although it does not exclude decadal  
336 periods with significant accumulation changes. Our results tend to show that the surface mass balance  
337 has changed slightly since the beginning of the 21<sup>st</sup> century. Despite this small change, this glacier can  
338 be considered to have been close to steady state conditions over the last 100 years.

339 In opposition to surface mass balance, englacial temperatures are strongly changing in response to  
340 atmospheric warming. This highlights the non-linear response of near-surface temperature to  
341 atmospheric forcing due a modified surface energy balance when surface melting occurs (Gilbert et  
342 al., 2014a). As surface melting events become more and more frequent, the energy absorbed by the  
343 glacier is largely enhanced, resulting in a strong warming signal observed in the borehole temperature  
344 profiles. Our simulation and inversion shows that the observed temperature profiles reflect a  
345 slowdown in the atmospheric warming rate, which is observed at lower elevation at both local and  
346 global scales. The slight near-surface temperature cooling trend inferred in our inversion (Fig. 9a) may  
347 indicate a negative feedback linked to increasing surface melting that could be superimposed on the  
348 atmospheric forcing. Indeed, the increasing refreezing rate could start to create impermeable ice layers  
349 that prevents meltwater to percolate deeply in the firn. As the refreezing would occur closer to the  
350 surface in this case, the energy added by latent heat would be lost in winter in comparison with the  
351 case where latent heat is released deeper, below an insulating snow layer. This effect would  
352 significantly limit the effect of meltwater refreezing on firn temperature. With the atmospheric  
353 warming rate currently increasing again, future observations will provide the opportunity to evaluate  
354 the efficiency of this potential feedback.

355

## 356 **5. Conclusions**

357

358 Our comparison of two Digital Elevation Models produced in 1993 and 2017 over 0.12 km<sup>2</sup> at Col du  
359 Dôme shows that ice thickness changes were very small (<7 m) over this period at this altitude (4250  
360 m a.s.l.) in the Mont Blanc area. Ice flow velocity measurements show that the horizontal velocities  
361 have decreased by about 11 %. This leads to a decrease in ice flux of 9.7%. Although the surface mass  
362 balance observations are not available over the whole period, the ice flux calculations suggest a  
363 decrease of surface mass balance. This is confirmed by the analysis of submergence velocities which  
364 decreased by 21 % between 1993 and 2017. The overall analysis suggests that surface mass balance  
365 might have decreased by about 10 % over this period. Given that ablation is almost negligible  
366 compared to snow accumulation (Gilbert et al., 2014a), the change in surface mass balance is likely  
367 due to less snow accumulation and consequently to a change in precipitation. This is consistent with  
368 the meteorological reanalysis and winter snow accumulation measurements performed at lower  
369 altitudes.

370 As opposed to thickness and surface mass balance changes, the englacial temperatures reveal strong  
371 changes. The englacial temperature averaged over the entire profile increased by 0.9 °C between 1994  
372 and 2017. Numerical modeling with meteorological input data shows that the temperature profile was  
373 already far from steady state in 1994 in response to a warming phase that started in 1980. The near-  
374 surface temperature warming over the last 3 decades propagated through to the glacier and reached the  
375 bedrock between 2005 and 2010. Finally, our borehole temperature inversion shows an air temperature  
376 change very similar to that observed at low elevations in the Alps, including a warming hiatus  
377 occurring during the early 2000's.

378 In the future, near-surface temperature warming should continue to propagate down into the glacier.  
379 This warming could affect the stability of cold alpine hanging glaciers located on steep slopes and  
380 currently frozen to their bed. The progressive changes in thermal regime of these high elevation  
381 glaciers cannot be detected from the surface.

382 For hanging glaciers with basal ice temperatures close to the melting point, ice flow velocity  
383 monitoring is recommended, particularly when glacier collapse could jeopardize life and property in  
384 the valley below.

385

386 **Data availability:** The englacial temperature data and DEM data can be accessed upon request by  
387 contacting Christian Vincent ([christian.vincent@univ-grenoble-alpes.fr](mailto:christian.vincent@univ-grenoble-alpes.fr)).

388

389 **Author contributions:** LP, PG, VM, PP, EL drilled the ice cores. OL, DS and CV performed the  
390 geophysical and geodetic measurements. AG performed the numerical modeling. CV supervised the  
391 study and wrote the paper. All co-authors contributed to discussion of the results.

392

393 **Competing interests:** the authors declare that they have no conflict of interest.

394

395 **Acknowledgements:**

396

397 This study was funded by the AQWA European program and Ice Memory project. 2016 ice coring  
398 was conducted with a lightweight ice coring system (<http://cryosphere.co>). We thank Y. Durand, G.  
399 Giraud and S. Morin (CNRMGAME/CEN, Météo France) for providing the SAFRAN data and  
400 meteorological data from Lyon-Bron. We would also like to thank everyone who helped in collecting  
401 data during the glacier field campaigns including data collected in the framework of GLACIOCLIM  
402 program. We thank the Editor Valentina Radic and the reviewers Jon Ove Hagen and Veijo Pohjola  
403 whose thorough comments and suggestions improved the quality of the manuscript.

404 We are grateful to H. Harder for reviewing the English.

405

406 **References**

407

408 Aschwanden, A., and Blatter, H.: Mathematical modeling and numerical simulation of polythermal  
409 glaciers, *J. Geophys. Res.*, 114, F01027, doi:10.1029/2008JF001028, 2009.

410

411 Berthier, E., Vincent, C., Magnússon, E., Gunnlaugsson, Á. Þ., Pitte, P., Le Meur, E., Masiokas, M.,  
412 Ruiz, L., Pálsson, F., Belart, J.M.C., and Wagnon, P.: Glacier topography and elevation changes from  
413 Pléiades sub-meter stereo images, *The Cryosphere*, 8, 2275–2291, doi:10.5194/tc-8-2275-2014, 2014.

414

415 Cuffey, K., and Paterson, W. B. S.: *The Physics of Glaciers*, 4th ed., Academic, Amsterdam, 2010.

416

417 Durand, Y., Laternser, M., Giraud, G., Etchevers, P., Lesaffre, B., and Mérindol, L.: Reanalysis of 44  
418 Yr of Climate in the French Alps (1958–2002): Methodology, Model Validation, Climatology, and  
419 Trends for Air Temperature and Precipitation, *J. Appl. Meteorol. Clim.*, 48, 429–449,  
420 <https://doi.org/10.1175/2008JAMC1808.1>, 2009.

421

422 Gardner, A.S., Moholdt, G., Cogley, J.G., Wouters, B., Arendt, A.A., Wahr, J., Berthier, E., Pfeffer,  
423 T., Kaser, G., Hock, R., Ligtenberg, S.R.M., Bolch, T., Sharp, M., Hagen, J.O., van den Broeke, M.  
424 R., and Paul, P.: A reconciled estimate of glacier contributions to sea level rise: 2003–2009, *Science*,  
425 340, 6134, 852–857, <https://doi:10.1126/science.1234532>, 2013.

426

427 Gilbert, A., Wagnon, P., Vincent, C., Ginot, P., and Funk, M.: Atmospheric warming at a high  
428 elevation tropical site revealed by englacial temperatures at Illimani, Bolivia (6340 m above sea level,  
429 16°S, 67°W), *J. Geophys. Res.*, 115, D10109, doi:10.1029/2009JD012961, 2010.

430

431 Gilbert, A., and Vincent, C.: Atmospheric temperature changes over the 20th century at very high  
432 elevations in the European Alps from englacial temperatures, *Geophys. Res. Lett.*, 40,  
433 doi:10.1002/grl.50401, 2013.

434

435 Gilbert A., Vincent, C., Six, D., Wagnon, P., Piard, L., and Ginot, P.: Modeling near-surface firn  
436 temperature in a cold accumulation zone (Col du Dôme, French Alps): from a physical to a semi-  
437 parameterized approach, *The Cryosphere*, 8, 689–703, doi:10.5194/tc-8-689-2014, 2014a.

438

439 Gilbert, A., Gagliardini, O., Vincent, C., and Wagnon, P.: A 3-D thermal regime model suitable for  
440 cold accumulation zones of polythermal mountain glaciers, *J. Geophys. Res.*, 119(9), 1876–1893,  
441 doi:10.1002/2014JF003199, 2014b.

442

443 Hoelzle, M., Darms, G., Lüthi, M.P., and Suter, S.: Evidence of accelerated englacial warming in the  
444 Monte Rosa area, Switzerland/Italy, *The Cryosphere*, 5, 231-243, doi:10.5194/tc-5-231-2011, 2011.  
445

446 Hooke, R.L.: *Principles of Glacier Mechanics*, Cambridge University Press, 429 p, 2005.  
447

448 Huss, M.: Extrapolating glacier mass balance to the mountain-range scale: The European Alps 1900-  
449 2010. 2012, *The Cryosphere*, 6, 713-727, doi:10.5194/tc-6-713-2012, 2012.  
450

451 Hutter, K.: *Theoretical Glaciology: Material Science of Ice and the Mechanics of Glaciers and Ice*  
452 *Sheets*, D. Reidel, Dordrecht, Netherlands, 1983.  
453

454 Lüthi, M., and Funk, M.: Modelling heat flow in a cold, high-altitude glacier: interpretation of  
455 measurements from Colle Gnifetti, Swiss Alps, *J. Glaciol.*, 47, 314-324, 2001.  
456

457 Meehl, G. A., Teng, H., and Arblaster, J.M.: Climate model simulations of the observed early-2000s  
458 hiatus of global warming, *Nature Climate Change*, 4(10), 898–902, doi:[10.1038/nclimate2357](https://doi.org/10.1038/nclimate2357), 2014.  
459

460 Narod, B.B. and Clarke, G.K.C.: Miniature high-power impulse transmitter for radio-echo sounding. *J.*  
461 *Glaciol.*, 40(134), 190-194, 1994.  
462

463 Oerlemans, J.: *Glaciers and Climate change*, Balkema Publishers, Lisse, 2001.  
464

465 Suter, S.: Dépouillement des sondages radar au Col du Dôme, Massif du Mont Blanc, du 1er au 5 juin  
466 1993, Travail de stage pratique réalisé sous la responsabilité de M. Funk et de W. Haeberli. Rapport  
467 non publié du VAW et de l'EPFZ de Zurich, 1993.  
468

469 Suter, S.: Cold firn and ice in the Monte Rosa and Mont Blanc areas (spatial occurrence, surface energy  
470 balance and climatic evidence), Ph.D. thesis, ETH Zurich, 2002.  
471

472 Thibert, E., Dkengne Sielenou, P., Vionnet, V., Eckert, N., and Vincent, C.: Causes of glacier melt  
473 extremes in the Alps since 1949, *Geophys. Res. Letters*, 45, <https://doi.org/10.1002/2017GL076333>,  
474 2018.  
475

476 Vincent, C., Vallon, M., Pinglot, J.F., Funk, M., and Reynaud, L.: Snow accumulation and ice flow at  
477 Dôme du Goûter (4300 m), Mont Blanc, French Alps, *J. Glaciol.*, 43, 513-521, Erratum (1998), *J.*  
478 *Glaciol.*, 44, 194, 1997.  
479

480 Vincent, C., Le Meur, E., Six, D., Funk, M., Hoelzle, M., and Preunkert, S.: Very high elevation Mont  
481 Blanc glaciated areas not affected by the 20th century climate change, *J. Geophys. Res.*, 112  
482 (D09120), doi:10.1029/2006JD007407, 2007a.  
483

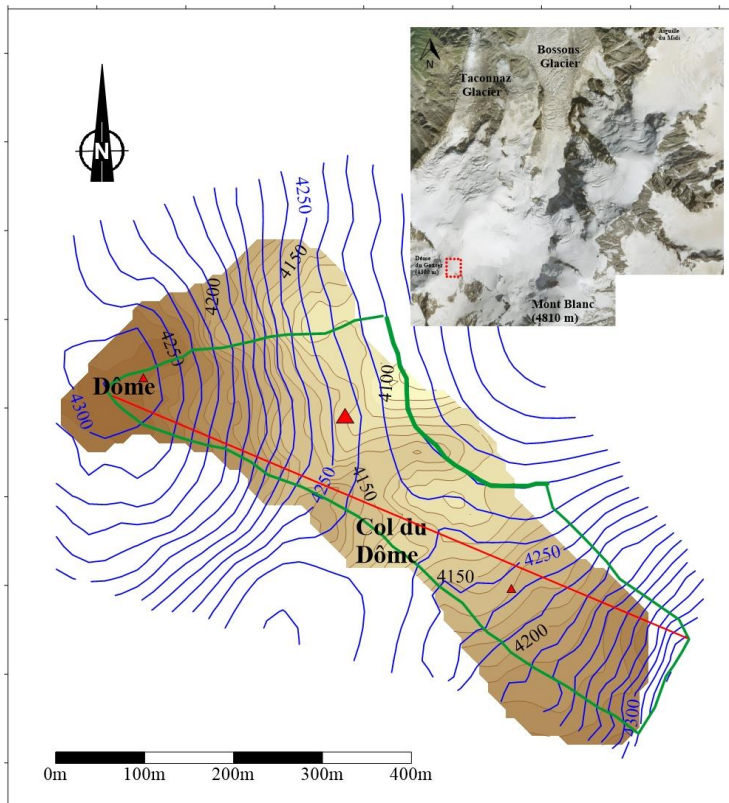
484 Vincent, C., Le Meur, E., Six, D., Possenti, P., Lefebvre, E., and Funk, M.: Climate warming revealed  
485 by englacial temperatures at Col du Dôme (4250 m, Mont-Blanc area), *Geophys. Res. Lett.*, 34  
486 (L16502), doi:10.1029/2007GL029933, 2007b.  
487

488 Vincent C., Harter, H., Gilbert, A., Berthier, E., and Six, D.: Future fluctuations of Mer de Glace,  
489 French Alps, assessed using a parameterized model calibrated with past thickness changes, *Annals of*  
490 *Glaciology*, 55 (66), doi:10.3189/2014AoG66A050, 2014  
491

492 Wagner, S.: Dredimensionale modellierung zweier Gletscher und deformations analyse von eisreichem  
493 permafrost, PhD thesis, ETH, Zurich, Dissertation 10659, 1994.  
494

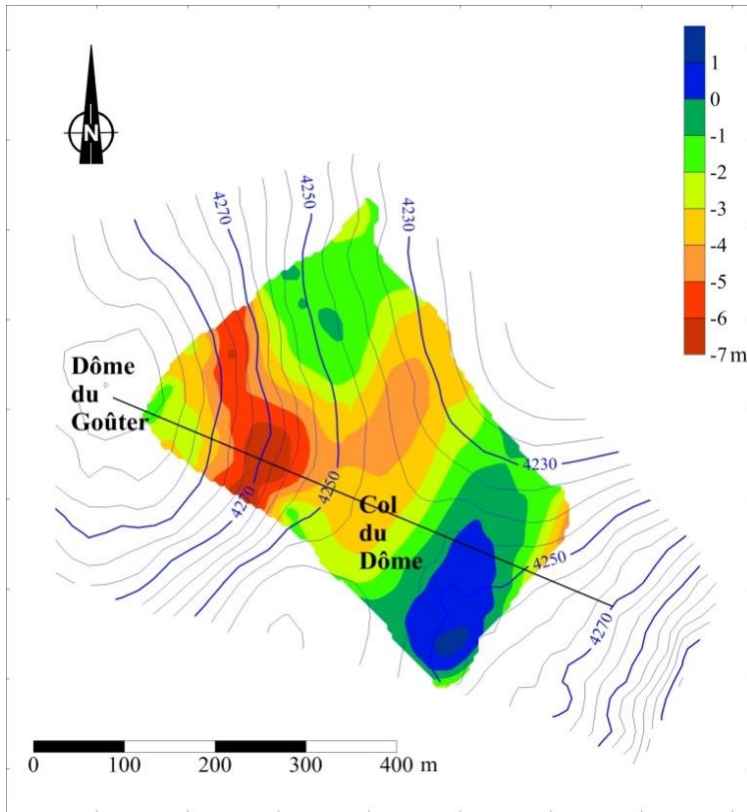
495 WGMS: Global glacier change bulletin no.1 (2012-2013), Zemp, M., Gärtner-Roer, Nussbaumer, S.  
496 U., Hüsler, F., Machgut, H., Mölg, N., Paul, F. and Hoelzle, M. (eds),  
497 ICSU(WDS)/IUGG(IASC)/UNEP/UNESCO/WMO, World Glacier Monitoring Service, Zürich,  
498 Switzerland, 230 pp, 2015.  
499

500 Zemp, M., Huss, M., Thibert, E., Eckert, N., McNabb, R., Huber, J., Barandun, M., Machguth, H.,  
501 Nussbaumer, S.U., Gärtner-Roer, I., Thomson, L., Paul, F., Maussion, F., Kutuzov, S., and Cogley,  
502 J.G.: Global glacier mass changes and their contributions to sea-level rise from 1961 to 2016,  
503 *Nature*, 568, 382–386, doi.org/10.1038/s41586-019-1071-0, 2019.  
504

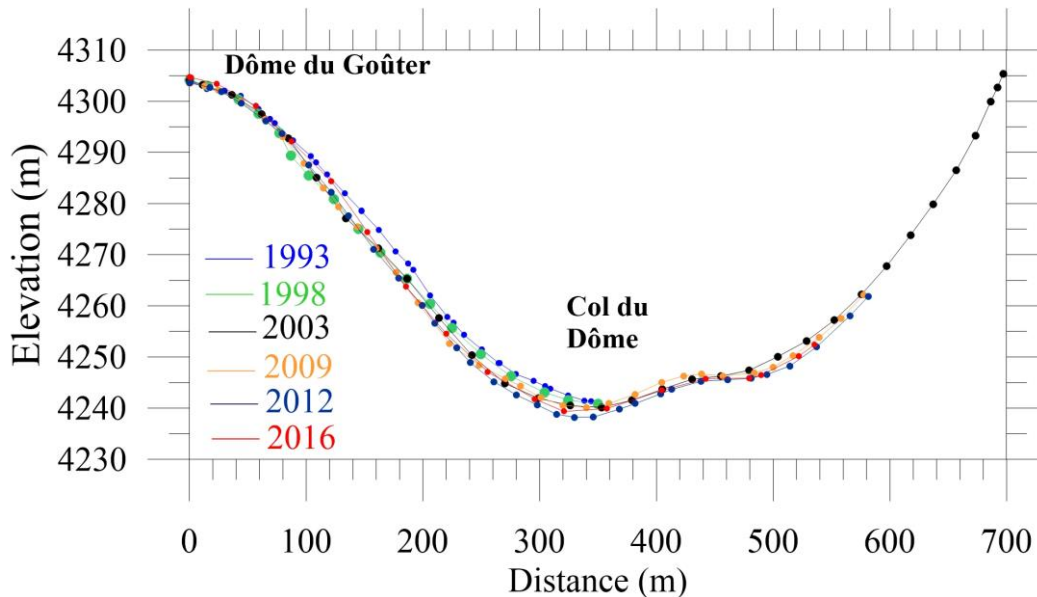


505  
 506 *Figure 1: Surface (blue) and bedrock (brown) digital elevation models of the Dôme du Goûter area.*  
 507 *Elevation differences between two contour lines are 5 and 10 m for the surface and bedrock*  
 508 *respectively. The large red triangle is the location of the core drilling and englacial temperature*  
 509 *measurement site for this study. The two other small red triangles correspond to the locations of the*  
 510 *previous englacial temperature measurement sites we used also for the temperature inversion. The*  
 511 *green line shows the boundaries of the drainage basin and the flux gate (thick line) through which the*  
 512 *ice flux change has been calculated. The red line shows the cross section used for altitude*  
 513 *measurements. Aerial picture from Institut Géographique National (©IGN).*

514

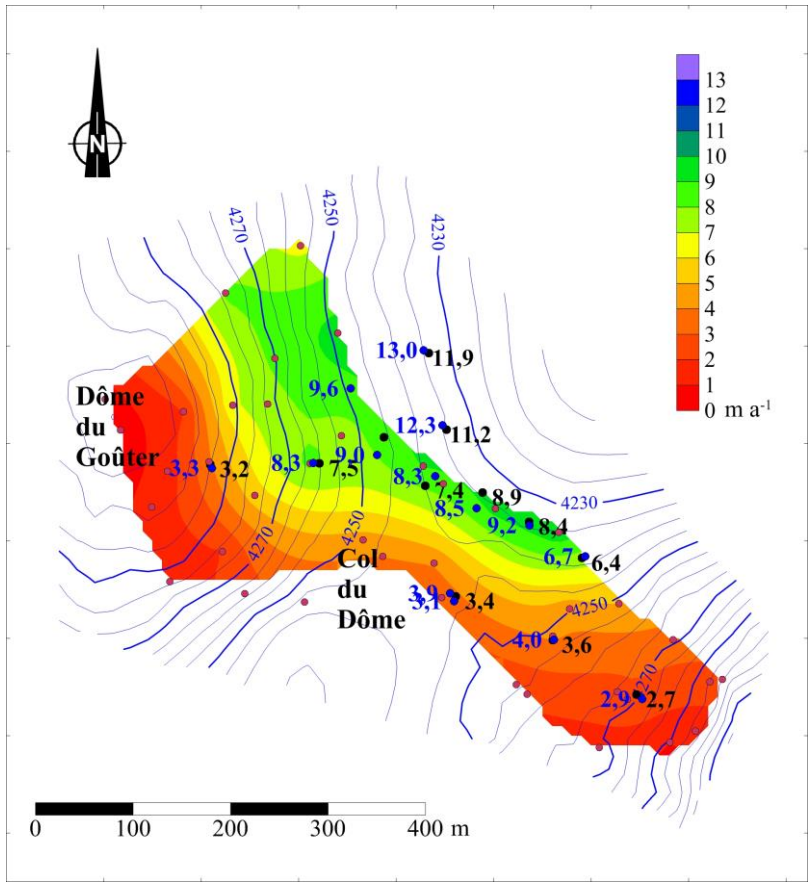


515  
 516 *Figure 2: Thickness changes (color scale) between 1993 and 2017. The contour lines of surface*  
 517 *topography correspond to the surface of 1993. The longitudinal cross section is shown by the thick*  
 518 *black line.*  
 519



520  
 521 *Figure 3: Longitudinal cross section from Dôme du Goûter to Col du Dôme obtained from DGPS*  
 522 *measurements performed in June 1993, May 1998, October 2003, September 2009, March 2012 and*  
 523 *August 2016.*  
 524





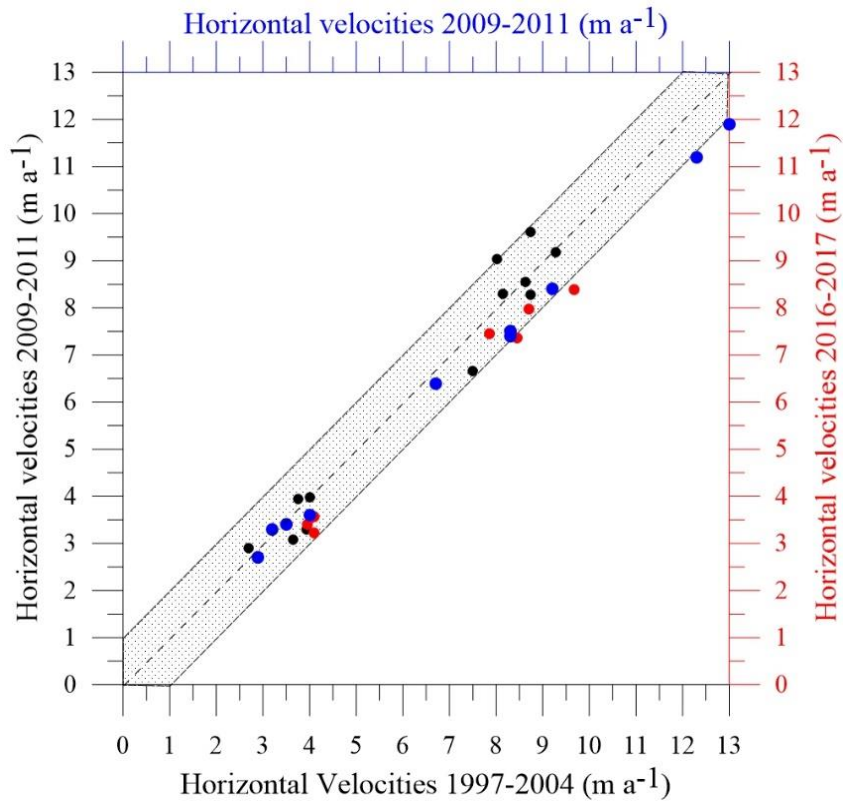
525

526

527 *Figure 4: Horizontal ice flow velocities ( $\text{m a}^{-1}$ ) observed between 1993 and 2004 (red dots and color*  
 528 *scale), between 2009 and 2011 (blue dots and values) and between 2016 and 2017 (black dots and*  
 529 *values).*

530

531



532

533 *Figure 5: Comparison of horizontal ice flow velocities between the periods 1997-2004, 2009-2011 and*

534 *2016-2017. The black dots correspond to the comparison between the 1997-2004 and 2009-2011*

535 *periods. The red dots correspond to the comparison between the 1997-2004 and 2016-2017 periods.*

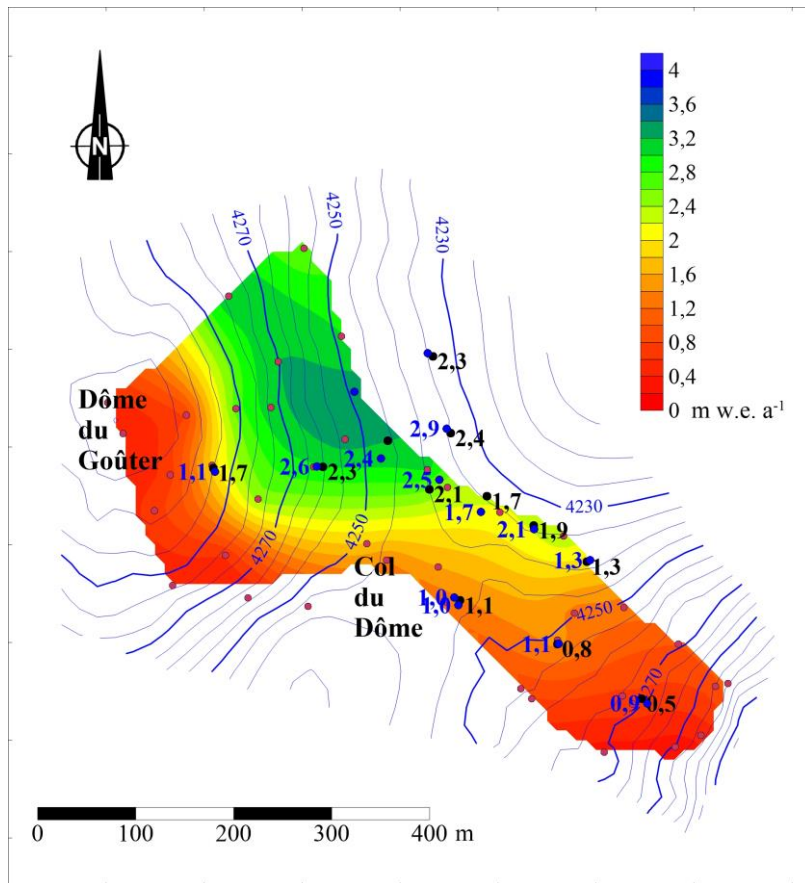
536 *The blue dots correspond to the comparison between the 2009-2011 and 2016-2017 periods. The gray*

537 *area corresponds to a difference of  $\pm 1 \text{ m a}^{-1}$  in relation to the bisector.*

538

539

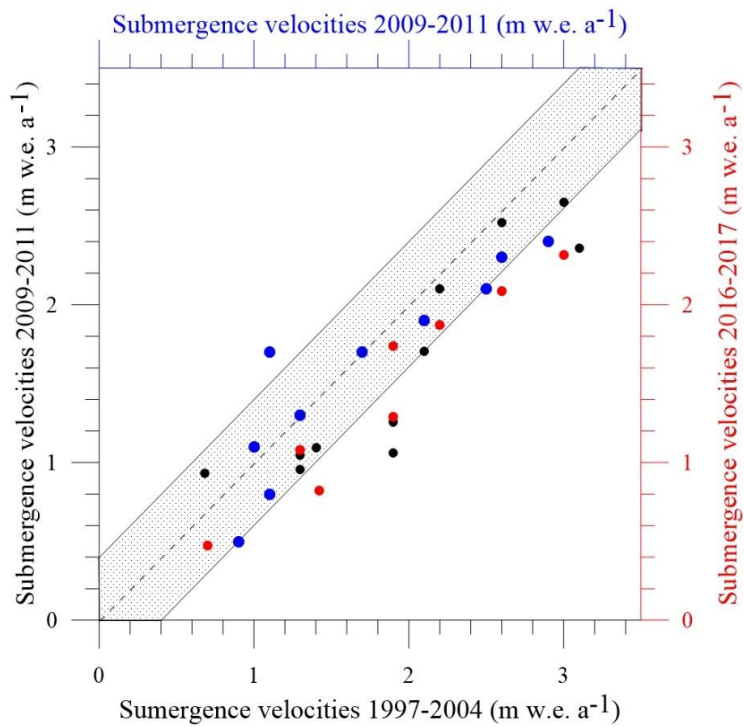
540



541

542 *Figure 6: Submergence velocities (m w.e. a<sup>-1</sup>) observed between 1997 and 2004 (red dots and color*  
 543 *scale), between 2009 and 2011 (blue dots and values) and between 2016 and 2017 (black dots and*  
 544 *values). For the sake of clarity, the submergence velocity values of the 1997-2004 period have not*  
 545 *been reported here.*

546



547

548 *Figure 7: Comparison of submergence velocities between 1997-2004, 2009-2011 and 2016-2017*

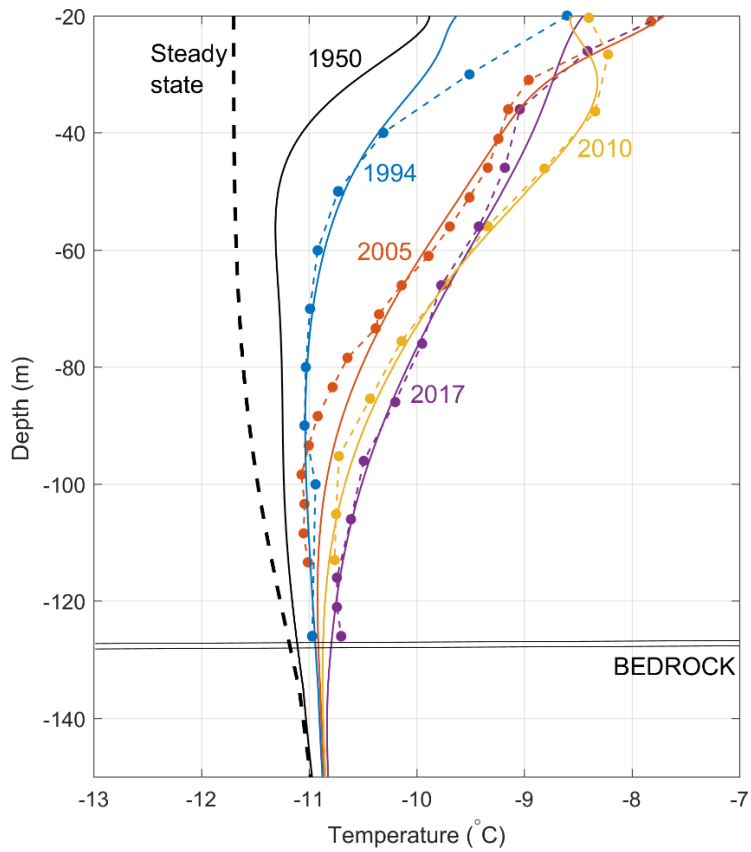
549 *periods. The black dots correspond to the comparison between the 1997-2004 and 2009-2011 periods.*

550 *The red dots correspond to the comparison between the 1997-2004 and 2016-2017 periods. The blue*

551 *dots correspond to the comparison between the 2009-2011 and 2016-2017 periods. The gray area*

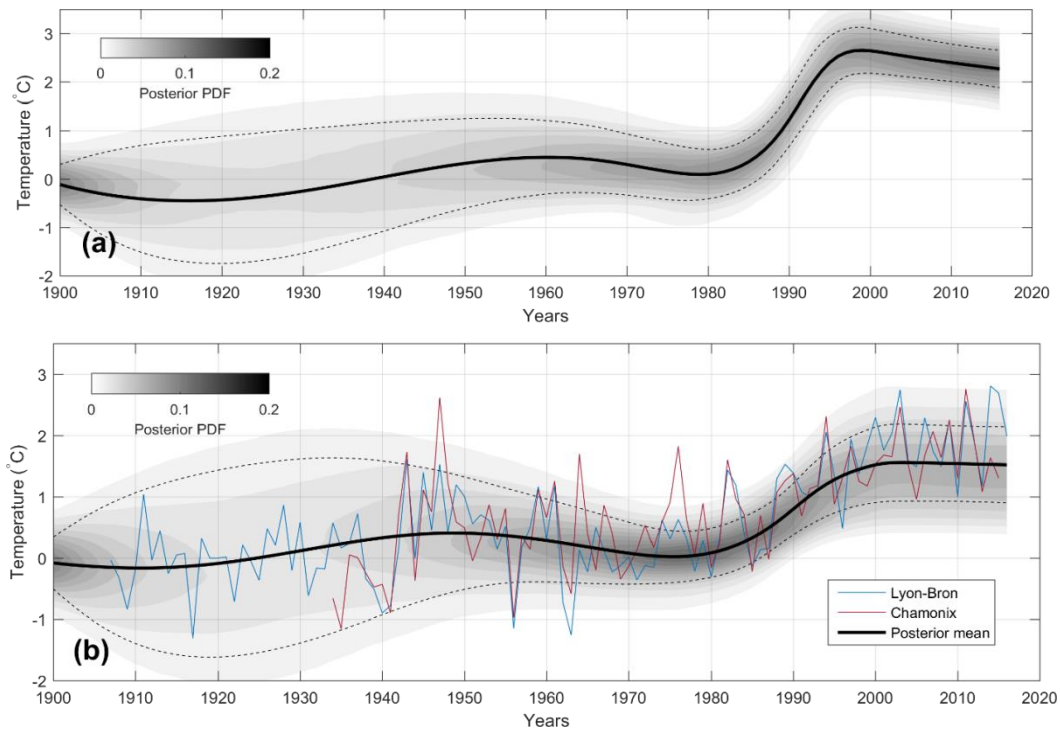
552 *corresponds to a difference of  $\pm 0.4$  m w.e. a<sup>-1</sup> in relation to the bisector.*

553



554  
 555  
 556  
 557  
 558  
 559  
 560

*Figure 8: Measured (dots) and modeled (continuous lines) englacial temperatures at the same location. The model is forced by air temperature data from Lyon-Bron meteorological station, located 200 km from the drilling site. The steady state profile is computed from a steady surface temperature and is used as the initial profile in 1907 for the model.*



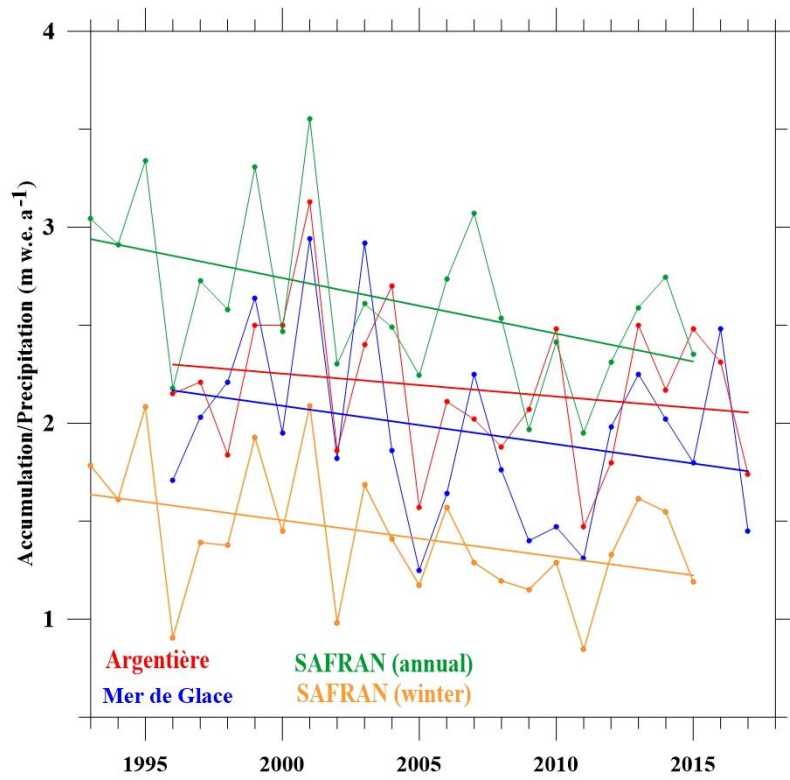
561

562 *Figure 9: (a) Temporal evolution of the near-surface temperature reconstructed at the drilling site*  
 563 *since 1900 (black bold line). (b) Past atmospheric temperature reconstructed from all measured*  
 564 *temperature profiles in the Col du Dôme area (black bold line) compared to Lyon-Bron (200 m a.s.l.,*  
 565 *blue line) and Chamonix (1000 m a.s.l., red line) temperature records. In both plots, the gray scale*  
 566 *represents the posterior probability function and the dashed line is its standard deviation.*

567

568

569



570

571 *Figure 10: Winter mass balance of Argentière and Mer de Glace glaciers over the period 1995-2017*  
 572 *and annual/winter precipitation (m w.e.) reanalysis over the period 1993-2015.*

573

574